# First measurement of the CP-violating phase in B0s→ decays

LHCb Collaboration ; et al ; Bernet, R ; Müller, K ; Steinkamp, O ; Straumann, U ; Vollhardt, A

Abstract: A first flavor-tagged measurement of the time-dependent CP-violating asymmetry in B0s→ decays is presented. In this decay channel, the CP-violating weak phase arises due to CP violation in the interference between B0s-B¯¯0s mixing and the b→ss¯s gluonic penguin decay amplitude. Using a sample of pp collision data corresponding to an integrated luminosity of 1.0 fb−1 and collected at a center-of-mass energy of 7 TeV with the LHCb detector, 880 B0s→ signal decays are obtained. The CP-violating phase is measured to be in the interval [−2.46,−0.76] rad at a 68% confidence level. The p value of the standard model prediction is 16%.

DOI: https://doi.org/10.1103/PhysRevLett.110.241802

EUROPEAN ORGANIZATION FOR NUCLEAR RESEARCH (CERN)

CERN-PH-EP-2013-046
LHCb-PAPER-2013-007
May 16, 2013



# First measurement of the *CP*-violating phase in $B_s^0 \to \phi\phi$ decays

The LHCb collaboration[†]

**Abstract**

A first flavour-tagged measurement of the time-dependent *CP*-violating asymmetry in $B_s^0 \to \phi\phi$ decays is presented. In this decay channel, the *CP*-violating weak phase arises due to *CP* violation in the interference between $B_s^0$-$\overline{B}_s^0$ mixing and the $b \to s\bar{s}s$ gluonic penguin decay amplitude. Using a sample of $pp$ collision data corresponding to an integrated luminosity of 1.0 fb$^{-1}$ and collected at a centre-of-mass energy of 7 TeV with the LHCb detector, 880 $B_s^0 \to \phi\phi$ signal decays are obtained. The *CP*-violating phase is measured to be in the interval $[-2.46, -0.76]$ rad at 68% confidence level. The p-value of the Standard Model prediction is 16%.

Submitted to Phys. Rev. Lett.



[†]Authors are listed on the following pages.

# LHCb collaboration

R. Aaij[40], C. Abellan Beteta[35,n], B. Adeva[36], M. Adinolfi[45], C. Adrover[6], A. Affolder[51], Z. Ajaltouni[5], J. Albrecht[9], F. Alessio[37], M. Alexander[50], S. Ali[40], G. Alkhazov[29], P. Alvarez Cartelle[36], A.A. Alves Jr[24,37], S. Amato[2], S. Amerio[21], Y. Amhis[7], L. Anderlini[17,f], J. Anderson[39], R. Andreassen[59], R.B. Appleby[53], O. Aquines Gutierrez[10], F. Archilli[18], A. Artamonov [34], M. Artuso[56], E. Aslanides[6], G. Auriemma[24,m], S. Bachmann[11], J.J. Back[47], C. Baesso[57], V. Balagura[30], W. Baldini[16], R.J. Barlow[53], C. Barschel[37], S. Barsuk[7], W. Barter[46], Th. Bauer[40], A. Bay[38], J. Beddow[50], F. Bedeschi[22], I. Bediaga[1], S. Belogurov[30], K. Belous[34], I. Belyaev[30], E. Ben-Haim[8], M. Benayoun[8], G. Bencivenni[18], S. Benson[49], J. Benton[45], A. Berezhnoy[31], R. Bernet[39], M.-O. Bettler[46], M. van Beuzekom[40], A. Bien[11], S. Bifani[12], T. Bird[53], A. Bizzeti[17,h], P.M. Bjørnstad[53], T. Blake[37], F. Blanc[38], J. Blouw[11], S. Blusk[56], V. Bocci[24], A. Bondar[33], N. Bondar[29], W. Bonivento[15], S. Borghi[53], A. Borgia[56], T.J.V. Bowcock[51], E. Bowen[39], C. Bozzi[16], T. Brambach[9], J. van den Brand[41], J. Bressieux[38], D. Brett[53], M. Britsch[10], T. Britton[56], N.H. Brook[45], H. Brown[51], I. Burducea[28], A. Bursche[39], G. Busetto[21,q], J. Buytaert[37], S. Cadeddu[15], O. Callot[7], M. Calvi[20,j], M. Calvo Gomez[35,n], A. Camboni[35], P. Campana[18,37], D. Campora Perez[37], A. Carbone[14,c], G. Carboni[23,k], R. Cardinale[19,i], A. Cardini[15], H. Carranza-Mejia[49], L. Carson[52], K. Carvalho Akiba[2], G. Casse[51], M. Cattaneo[37], Ch. Cauet[9], M. Charles[54], Ph. Charpentier[37], P. Chen[3,38], N. Chiapolini[39], M. Chrzaszcz [25], K. Ciba[37], X. Cid Vidal[37], G. Ciezarek[52], P.E.L. Clarke[49], M. Clemencic[37], H.V. Cliff[46], J. Closier[37], C. Coca[28], V. Coco[40], J. Cogan[6], E. Cogneras[5], P. Collins[37], A. Comerma-Montells[35], A. Contu[15], A. Cook[45], M. Coombes[45], S. Coquereau[8], G. Corti[37], B. Couturier[37], G.A. Cowan[49], D. Craik[47], S. Cunliffe[52], R. Currie[49], C. D'Ambrosio[37], P. David[8], P.N.Y. David[40], A. Davis[59], I. De Bonis[4], K. De Bruyn[40], S. De Capua[53], M. De Cian[39], J.M. De Miranda[1], L. De Paula[2], W. De Silva[59], P. De Simone[18], D. Decamp[4], M. Deckenhoff[9], L. Del Buono[8], D. Derkach[14], O. Deschamps[5], F. Dettori[41], A. Di Canto[11], H. Dijkstra[37], M. Dogaru[28], S. Donleavy[51], F. Dordei[11], A. Dosil Suárez[36], D. Dossett[47], A. Dovbnya[42], F. Dupertuis[38], R. Dzhelyadin[34], A. Dziurda[25], A. Dzyuba[29], S. Easo[48,37], U. Egede[52], V. Egorychev[30], S. Eidelman[33], D. van Eijk[40], S. Eisenhardt[49], U. Eitschberger[9], R. Ekelhof[9], L. Eklund[50,37], I. El Rifai[5], Ch. Elsasser[39], D. Elsby[44], A. Falabella[14,e], C. Färber[11], G. Fardell[49], C. Farinelli[40], S. Farry[12], V. Fave[38], D. Ferguson[49], V. Fernandez Albor[36], F. Ferreira Rodrigues[1], M. Ferro-Luzzi[37], S. Filippov[32], C. Fitzpatrick[37], M. Fontana[10], F. Fontanelli[19,i], R. Forty[37], O. Francisco[2], M. Frank[37], C. Frei[37], M. Frosini[17,f], S. Furcas[20], E. Furfaro[23], A. Gallas Torreira[36], D. Galli[14,c], M. Gandelman[2], P. Gandini[56], Y. Gao[3], J. Garofoli[56], P. Garosi[53], J. Garra Tico[46], L. Garrido[35], C. Gaspar[37], R. Gauld[54], E. Gersabeck[11], M. Gersabeck[53], T. Gershon[47,37], Ph. Ghez[4], V. Gibson[46], V.V. Gligorov[37], C. Göbel[57], D. Golubkov[30], A. Golutvin[52,30,37], A. Gomes[2], H. Gordon[54], M. Grabalosa Gándara[5], R. Graciani Diaz[35], L.A. Granado Cardoso[37], E. Graugés[35], G. Graziani[17], A. Grecu[28], E. Greening[54], S. Gregson[46], O. Grünberg[58], B. Gui[56], E. Gushchin[32], Yu. Guz[34,37], T. Gys[37], C. Hadjivasiliou[56], G. Haefeli[38], C. Haen[37], S.C. Haines[46], S. Hall[52], T. Hampson[45], S. Hansmann-Menzemer[11], N. Harnew[54], S.T. Harnew[45], J. Harrison[53], T. Hartmann[58], J. He[37], V. Heijne[40], K. Hennessy[51], P. Henrard[5], J.A. Hernando Morata[36], E. van Herwijnen[37], E. Hicks[51], D. Hill[54], M. Hoballah[5], C. Hombach[53], P. Hopchev[4], W. Hulsbergen[40], P. Hunt[54], T. Huse[51], N. Hussain[54], D. Hutchcroft[51], D. Hynds[50], V. Iakovenko[43], M. Idzik[26], P. Ilten[12], R. Jacobsson[37], A. Jaeger[11], E. Jans[40], P. Jaton[38],

F. Jing[3], M. John[54], D. Johnson[54], C.R. Jones[46], B. Jost[37], M. Kaballo[9], S. Kandybei[42], M. Karacson[37], T.M. Karbach[37], I.R. Kenyon[44], U. Kerzel[37], T. Ketel[41], A. Keune[38], B. Khanji[20], O. Kochebina[7], I. Komarov[38], R.F. Koopman[41], P. Koppenburg[40], M. Korolev[31], A. Kozlinskiy[40], L. Kravchuk[32], K. Kreplin[11], M. Kreps[47], G. Krocker[11], P. Krokovny[33], F. Kruse[9], M. Kucharczyk[20,25,j], V. Kudryavtsev[33], T. Kvaratskheliya[30,37], V.N. La Thi[38], D. Lacarrere[37], G. Lafferty[53], A. Lai[15], D. Lambert[49], R.W. Lambert[41], E. Lanciotti[37], G. Lanfranchi[18,37], C. Langenbruch[37], T. Latham[47], C. Lazzeroni[44], R. Le Gac[6], J. van Leerdam[40], J.-P. Lees[4], R. Lefèvre[5], A. Leflat[31], J. Lefrançois[7], S. Leo[22], O. Leroy[6], B. Leverington[11], Y. Li[3], L. Li Gioi[5], M. Liles[51], R. Lindner[37], C. Linn[11], B. Liu[3], G. Liu[37], S. Lohn[37], I. Longstaff[50], J.H. Lopes[2], E. Lopez Asamar[35], N. Lopez-March[38], H. Lu[3], D. Lucchesi[21,q], J. Luisier[38], H. Luo[49], F. Machefert[7], I.V. Machikhiliyan[4,30], F. Maciuc[28], O. Maev[29,37], S. Malde[54], G. Manca[15,d], G. Mancinelli[6], U. Marconi[14], R. Märki[38], J. Marks[11], G. Martellotti[24], A. Martens[8], L. Martin[54], A. Martín Sánchez[7], M. Martinelli[40], D. Martinez Santos[41], D. Martins Tostes[2], A. Massafferri[1], R. Matev[37], Z. Mathe[37], C. Matteuzzi[20], E. Maurice[6], A. Mazurov[16,32,37,e], J. McCarthy[44], R. McNulty[12], A. Mcnab[53], B. Meadows[59,54], F. Meier[9], M. Meissner[11], M. Merk[40], D.A. Milanes[8], M.-N. Minard[4], J. Molina Rodriguez[57], S. Monteil[5], D. Moran[53], P. Morawski[25], M.J. Morello[22,s], R. Mountain[56], I. Mous[40], F. Muheim[49], K. Müller[39], R. Muresan[28], B. Muryn[26], B. Muster[38], P. Naik[45], T. Nakada[38], R. Nandakumar[48], I. Nasteva[1], M. Needham[49], N. Neufeld[37], A.D. Nguyen[38], T.D. Nguyen[38], C. Nguyen-Mau[38,p], M. Nicol[7], V. Niess[5], R. Niet[9], N. Nikitin[31], T. Nikodem[11], A. Nomerotski[54], A. Novoselov[34], A. Oblakowska-Mucha[26], V. Obraztsov[34], S. Oggero[40], S. Ogilvy[50], O. Okhrimenko[43], R. Oldeman[15,d], M. Orlandea[28], J.M. Otalora Goicochea[2], P. Owen[52], A. Oyanguren [35,o], B.K. Pal[56], A. Palano[13,b], M. Palutan[18], J. Panman[37], A. Papanestis[48], M. Pappagallo[50], C. Parkes[53], C.J. Parkinson[52], G. Passaleva[17], G.D. Patel[51], M. Patel[52], G.N. Patrick[48], C. Patrignani[19,i], C. Pavel-Nicorescu[28], A. Pazos Alvarez[36], A. Pellegrino[40], G. Penso[24,l], M. Pepe Altarelli[37], S. Perazzini[14,c], D.L. Perego[20,j], E. Perez Trigo[36], A. Pérez-Calero Yzquierdo[35], P. Perret[5], M. Perrin-Terrin[6], G. Pessina[20], K. Petridis[52], A. Petrolini[19,i], A. Phan[56], E. Picatoste Olloqui[35], B. Pietrzyk[4], T. Pilař[47], D. Pinci[24], S. Playfer[49], M. Plo Casasus[36], F. Polci[8], G. Polok[25], A. Poluektov[47,33], E. Polycarpo[2], D. Popov[10], B. Popovici[28], C. Potterat[35], A. Powell[54], J. Prisciandaro[38], V. Pugatch[43], A. Puig Navarro[38], G. Punzi[22,r], W. Qian[4], J.H. Rademacker[45], B. Rakotomiaramanana[38], M.S. Rangel[2], I. Raniuk[42], N. Rauschmayr[37], G. Raven[41], S. Redford[54], M.M. Reid[47], A.C. dos Reis[1], S. Ricciardi[48], A. Richards[52], K. Rinnert[51], V. Rives Molina[35], D.A. Roa Romero[5], P. Robbe[7], E. Rodrigues[53], P. Rodriguez Perez[36], S. Roiser[37], V. Romanovsky[34], A. Romero Vidal[36], J. Rouvinet[38], T. Ruf[37], F. Ruffini[22], H. Ruiz[35], P. Ruiz Valls[35,o], G. Sabatino[24,k], J.J. Saborido Silva[36], N. Sagidova[29], P. Sail[50], B. Saitta[15,d], C. Salzmann[39], B. Sanmartin Sedes[36], M. Sannino[19,i], R. Santacesaria[24], C. Santamarina Rios[36], E. Santovetti[23,k], M. Sapunov[6], A. Sarti[18,l], C. Satriano[24,m], A. Satta[23], M. Savrie[16,e], D. Savrina[30,31], P. Schaack[52], M. Schiller[41], H. Schindler[37], M. Schlupp[9], M. Schmelling[10], B. Schmidt[37], O. Schneider[38], A. Schopper[37], M.-H. Schune[7], R. Schwemmer[37], B. Sciascia[18], A. Sciubba[24], M. Seco[36], A. Semennikov[30], K. Senderowska[26], I. Sepp[52], N. Serra[39], J. Serrano[6], P. Seyfert[11], M. Shapkin[34], I. Shapoval[42], P. Shatalov[30], Y. Shcheglov[29], T. Shears[51,37], L. Shekhtman[33], O. Shevchenko[42], V. Shevchenko[30], A. Shires[52], R. Silva Coutinho[47], T. Skwarnicki[56], N.A. Smith[51], E. Smith[54,48], M. Smith[53], M.D. Sokoloff[59], F.J.P. Soler[50], F. Soomro[18], D. Souza[45], B. Souza De Paula[2], B. Spaan[9],

A. Sparkes[49], P. Spradlin[50], F. Stagni[37], S. Stahl[11], O. Steinkamp[39], S. Stoica[28], S. Stone[56], B. Storaci[39], M. Straticiuc[28], U. Straumann[39], V.K. Subbiah[37], S. Swientek[9], V. Syropoulos[41], M. Szczekowski[27], P. Szczypka[38,37], T. Szumlak[26], S. T'Jampens[4], M. Teklishyn[7], E. Teodorescu[28], F. Teubert[37], C. Thomas[54], E. Thomas[37], J. van Tilburg[11], V. Tisserand[4], M. Tobin[39], S. Tolk[41], D. Tonelli[37], S. Topp-Joergensen[54], N. Torr[54], E. Tournefier[4,52], S. Tourneur[38], M.T. Tran[38], M. Tresch[39], A. Tsaregorodtsev[6], P. Tsopelas[40], N. Tuning[40], M. Ubeda Garcia[37], A. Ukleja[27], D. Urner[53], U. Uwer[11], V. Vagnoni[14], G. Valenti[14], R. Vazquez Gomez[35], P. Vazquez Regueiro[36], S. Vecchi[16], J.J. Velthuis[45], M. Veltri[17,g], G. Veneziano[38], M. Vesterinen[37], B. Viaud[7], D. Vieira[2], X. Vilasis-Cardona[35,n], A. Vollhardt[39], D. Volyanskyy[10], D. Voong[45], A. Vorobyev[29], V. Vorobyev[33], C. Voß[58], H. Voss[10], R. Waldi[58], R. Wallace[12], S. Wandernoth[11], J. Wang[56], D.R. Ward[46], N.K. Watson[44], A.D. Webber[53], D. Websdale[52], M. Whitehead[47], J. Wicht[37], J. Wiechczynski[25], D. Wiedner[11], L. Wiggers[40], G. Wilkinson[54], M.P. Williams[47,48], M. Williams[55], F.F. Wilson[48], J. Wishahi[9], M. Witek[25], S.A. Wotton[46], S. Wright[46], S. Wu[3], K. Wyllie[37], Y. Xie[49,37], F. Xing[54], Z. Xing[56], Z. Yang[3], R. Young[49], X. Yuan[3], O. Yushchenko[34], M. Zangoli[14], M. Zavertyaev[10,a], F. Zhang[3], L. Zhang[56], W.C. Zhang[12], Y. Zhang[3], A. Zhelezov[11], A. Zhokhov[30], L. Zhong[3], A. Zvyagin[37].

[1] *Centro Brasileiro de Pesquisas Físicas (CBPF), Rio de Janeiro, Brazil*
[2] *Universidade Federal do Rio de Janeiro (UFRJ), Rio de Janeiro, Brazil*
[3] *Center for High Energy Physics, Tsinghua University, Beijing, China*
[4] *LAPP, Université de Savoie, CNRS/IN2P3, Annecy-Le-Vieux, France*
[5] *Clermont Université, Université Blaise Pascal, CNRS/IN2P3, LPC, Clermont-Ferrand, France*
[6] *CPPM, Aix-Marseille Université, CNRS/IN2P3, Marseille, France*
[7] *LAL, Université Paris-Sud, CNRS/IN2P3, Orsay, France*
[8] *LPNHE, Université Pierre et Marie Curie, Université Paris Diderot, CNRS/IN2P3, Paris, France*
[9] *Fakultät Physik, Technische Universität Dortmund, Dortmund, Germany*
[10] *Max-Planck-Institut für Kernphysik (MPIK), Heidelberg, Germany*
[11] *Physikalisches Institut, Ruprecht-Karls-Universität Heidelberg, Heidelberg, Germany*
[12] *School of Physics, University College Dublin, Dublin, Ireland*
[13] *Sezione INFN di Bari, Bari, Italy*
[14] *Sezione INFN di Bologna, Bologna, Italy*
[15] *Sezione INFN di Cagliari, Cagliari, Italy*
[16] *Sezione INFN di Ferrara, Ferrara, Italy*
[17] *Sezione INFN di Firenze, Firenze, Italy*
[18] *Laboratori Nazionali dell'INFN di Frascati, Frascati, Italy*
[19] *Sezione INFN di Genova, Genova, Italy*
[20] *Sezione INFN di Milano Bicocca, Milano, Italy*
[21] *Sezione INFN di Padova, Padova, Italy*
[22] *Sezione INFN di Pisa, Pisa, Italy*
[23] *Sezione INFN di Roma Tor Vergata, Roma, Italy*
[24] *Sezione INFN di Roma La Sapienza, Roma, Italy*
[25] *Henryk Niewodniczanski Institute of Nuclear Physics Polish Academy of Sciences, Kraków, Poland*
[26] *AGH University of Science and Technology, Kraków, Poland*
[27] *National Center for Nuclear Research (NCBJ), Warsaw, Poland*
[28] *Horia Hulubei National Institute of Physics and Nuclear Engineering, Bucharest-Magurele, Romania*
[29] *Petersburg Nuclear Physics Institute (PNPI), Gatchina, Russia*
[30] *Institute of Theoretical and Experimental Physics (ITEP), Moscow, Russia*
[31] *Institute of Nuclear Physics, Moscow State University (SINP MSU), Moscow, Russia*
[32] *Institute for Nuclear Research of the Russian Academy of Sciences (INR RAN), Moscow, Russia*
[33] *Budker Institute of Nuclear Physics (SB RAS) and Novosibirsk State University, Novosibirsk, Russia*

[34] *Institute for High Energy Physics (IHEP), Protvino, Russia*
[35] *Universitat de Barcelona, Barcelona, Spain*
[36] *Universidad de Santiago de Compostela, Santiago de Compostela, Spain*
[37] *European Organization for Nuclear Research (CERN), Geneva, Switzerland*
[38] *Ecole Polytechnique Fédérale de Lausanne (EPFL), Lausanne, Switzerland*
[39] *Physik-Institut, Universität Zürich, Zürich, Switzerland*
[40] *Nikhef National Institute for Subatomic Physics, Amsterdam, The Netherlands*
[41] *Nikhef National Institute for Subatomic Physics and VU University Amsterdam, Amsterdam, The Netherlands*
[42] *NSC Kharkiv Institute of Physics and Technology (NSC KIPT), Kharkiv, Ukraine*
[43] *Institute for Nuclear Research of the National Academy of Sciences (KINR), Kyiv, Ukraine*
[44] *University of Birmingham, Birmingham, United Kingdom*
[45] *H.H. Wills Physics Laboratory, University of Bristol, Bristol, United Kingdom*
[46] *Cavendish Laboratory, University of Cambridge, Cambridge, United Kingdom*
[47] *Department of Physics, University of Warwick, Coventry, United Kingdom*
[48] *STFC Rutherford Appleton Laboratory, Didcot, United Kingdom*
[49] *School of Physics and Astronomy, University of Edinburgh, Edinburgh, United Kingdom*
[50] *School of Physics and Astronomy, University of Glasgow, Glasgow, United Kingdom*
[51] *Oliver Lodge Laboratory, University of Liverpool, Liverpool, United Kingdom*
[52] *Imperial College London, London, United Kingdom*
[53] *School of Physics and Astronomy, University of Manchester, Manchester, United Kingdom*
[54] *Department of Physics, University of Oxford, Oxford, United Kingdom*
[55] *Massachusetts Institute of Technology, Cambridge, MA, United States*
[56] *Syracuse University, Syracuse, NY, United States*
[57] *Pontifícia Universidade Católica do Rio de Janeiro (PUC-Rio), Rio de Janeiro, Brazil, associated to* [2]
[58] *Institut für Physik, Universität Rostock, Rostock, Germany, associated to* [11]
[59] *University of Cincinnati, Cincinnati, OH, United States, associated to* [56]

[a] *P.N. Lebedev Physical Institute, Russian Academy of Science (LPI RAS), Moscow, Russia*
[b] *Università di Bari, Bari, Italy*
[c] *Università di Bologna, Bologna, Italy*
[d] *Università di Cagliari, Cagliari, Italy*
[e] *Università di Ferrara, Ferrara, Italy*
[f] *Università di Firenze, Firenze, Italy*
[g] *Università di Urbino, Urbino, Italy*
[h] *Università di Modena e Reggio Emilia, Modena, Italy*
[i] *Università di Genova, Genova, Italy*
[j] *Università di Milano Bicocca, Milano, Italy*
[k] *Università di Roma Tor Vergata, Roma, Italy*
[l] *Università di Roma La Sapienza, Roma, Italy*
[m] *Università della Basilicata, Potenza, Italy*
[n] *LIFAELS, La Salle, Universitat Ramon Llull, Barcelona, Spain*
[o] *IFIC, Universitat de Valencia-CSIC, Valencia, Spain*
[p] *Hanoi University of Science, Hanoi, Viet Nam*
[q] *Università di Padova, Padova, Italy*
[r] *Università di Pisa, Pisa, Italy*
[s] *Scuola Normale Superiore, Pisa, Italy*

The $B_s^0 \to \phi\phi$ decay is forbidden at tree level in the Standard Model (SM) and proceeds via a gluonic $b \to s\bar{s}s$ penguin process. Hence, this channel provides an excellent probe of new heavy particles entering the penguin quantum loops [1–3]. Generally, *CP* violation in the SM is governed by a single phase in the Cabibbo-Kobayashi-Maskawa quark mixing matrix [4]. The interference between the $B_s^0$-$\overline{B}_s^0$ oscillation and decay amplitudes leads to a *CP* asymmetry in the decay time distributions of $B_s^0$ and $\overline{B}_s^0$ mesons, which is characterised by a *CP*-violating weak phase. The SM predicts this phase to be small. Due to different decay amplitudes the actual value is dependent on the $B_s^0$ decay channel. For $B_s^0 \to J/\psi\phi$, which proceeds via a $b \to c\bar{c}s$ transition, the SM prediction of the weak phase is given by $-2\arg\left(-V_{ts}V_{tb}^*/V_{cs}V_{cb}^*\right) = -0.036 \pm 0.002$ rad [5]. The LHCb collaboration recently measured the weak phase in this decay to be $0.068 \pm 0.091(\text{stat}) \pm 0.011(\text{syst})$ rad [6], which is consistent with the SM and places stringent constraints on *CP* violation in $B_s^0$-$\overline{B}_s^0$ oscillations [7]. In the SM, the phase in the $B_s^0 \to \phi\phi$ decay, $\phi_s$, is expected to be close to zero due to a cancellation of the phases arising from $B_s^0$-$\overline{B}_s^0$ oscillations and decay [8]. Calculations using QCD factorization provide an upper limit of 0.02 rad for $|\phi_s|$ [1–3].

In this Letter, we present the first measurement of the *CP*-violating phase in $B_s^0 \to \phi\phi$ decays. Charge conjugate states are implied. The result is based on *pp* collision data corresponding to an integrated luminosity of 1.0 fb$^{-1}$ and collected by the LHCb experiment in 2011 at a centre-of-mass energy of 7 TeV. This data sample was previously used for a time-integrated measurement of the polarisation amplitudes and triple product asymmetries in the same decay mode [9]. The analysis reported here improves the selection efficiency, measures the $B_s^0$ decay time and identifies the flavour of the $B_s^0$ meson at production. This allows a study of *CP* violation in the interference between mixing and decay to be performed. It is necessary to disentangle the *CP*-even longitudinal ($A_0$), *CP*-even transverse ($A_\parallel$), and *CP*-odd transverse ($A_\perp$) polarisations of the $\phi\phi$ final state by measuring the distributions of the helicity angles [9].

The LHCb detector is a forward spectrometer at the Large Hadron Collider covering the pseudorapidity range $2 < \eta < 5$ and is described in detail in Ref. [10]. Events are selected by a hardware trigger, which selects hadron or muon candidates with high transverse energy or momentum ($p_{\rm T}$), followed by a two stage software trigger [11]. In the software trigger, $B_s^0 \to \phi\phi$ candidates are selected either by identifying events containing a pair of oppositely charged kaons with an invariant mass close to that of the $\phi$ meson or by using a topological *b*-hadron trigger. In the simulation, *pp* collisions are generated using Pythia 6.4 [12], with a specific LHCb configuration [13]. Decays of hadronic particles are described by EvtGen [14] and the detector response is implemented using the Geant4 toolkit [15] as described in Ref. [16].

The $B_s^0 \to \phi\phi$ decays are reconstructed by combining two $\phi$ meson candidates that decay into the $K^+K^-$ final state. Kaon candidates are required to have $p_{\rm T} > 0.5$ GeV/$c$, and an impact parameter (IP) $\chi^2$ larger than 16 with respect to the primary vertex (PV), where the IP $\chi^2$ is defined as the difference between the $\chi^2$ of the PV reconstructed with and without the considered track. Candidates must also be identified as kaons using the ring-imaging Cherenkov detectors [17], by requiring that the difference in the global likelihood between the kaon and pion mass hypotheses ($\Delta\ln\mathcal{L}_{K\pi} \equiv \ln\mathcal{L}_K - \ln\mathcal{L}_\pi$) be

larger than $-5$. Both $\phi$ meson candidates must have a reconstructed mass, $m_{KK}$, of the kaon pair within 20 MeV/$c^2$ of the known mass of the $\phi$ meson, a transverse momentum ($p_{\rm T}^{\phi}$) larger than 0.9 GeV/$c$ and a product, $p_{\rm T}^{\phi 1} p_{\rm T}^{\phi 2} > 2$ GeV$^2/c^2$. The $\chi^2$ per degree of freedom (ndf) of the vertex fit for both $\phi$ meson candidates and the $B_s^0$ candidate is required to be smaller than 25. Using the above criteria, 17 575 candidates are selected in the invariant four-kaon mass range $5100 < m_{KKKK} < 5600$ MeV/$c^2$.

A boosted decision tree (BDT) [18] is used to separate signal from background. The six observables used as input to the BDT are: $p_{\rm T}$, $\eta$ and $\chi^2$/ndf of the vertex fit for the $B_s^0$ candidate and the cosine of the angle between the $B_s^0$ momentum and the direction of flight from the closest primary vertex to the decay vertex, in addition to the smallest $p_{\rm T}$ and the largest track $\chi^2$/ndf of the kaon tracks. The BDT is trained using simulated $B_s^0 \to \phi\phi$ signal events and background from the data where at least one of the $\phi$ candidates has invariant mass in the range $20 < |m_{KK} - m_{\phi}| < 25$ MeV/$c^2$.

The *sPlot* technique [19, 20] is used to assign a signal weight to each $B_s^0 \to \phi\phi$ candidate. Using the four-kaon mass as the discriminating variable, the distributions of the signal components for the $B_s^0$ decay time and helicity angles can be determined in the data sample. The sensitivity to $\phi_s$ is optimised taking into account the signal purity and the flavour tagging performance. The final selection of $B_s^0 \to \phi\phi$ candidates based on this optimisation is required to have a BDT output larger than 0.1, $\Delta \ln \mathcal{L}_{K\pi} > -3$ for each kaon and $|m_{KK} - m_{\phi}| < 15$ MeV/$c^2$ for each $\phi$ candidate.

In total, 1182 $B_s^0 \to \phi\phi$ candidates are selected. Figure 1 shows the four-kaon invariant mass distribution for the selected events. Using an unbinned extended maximum likelihood fit, a signal yield of $880 \pm 31$ events is obtained. In this fit, the $B_s^0 \to \phi\phi$ signal component is modelled by two Gaussian functions with a common mean. The width of the first Gaussian component is measured to be $12.9 \pm 0.5$ MeV/$c^2$, in agreement with the expectation from simulation. The relative fraction and width of the second Gaussian component are fixed from simulation to values of 0.785 and 29.5 MeV/$c^2$, respectively, in order to ensure a good quality fit. Combinatorial background is modelled using an exponential function which is allowed to vary in the fit. Contributions from specific backgrounds such as $B^0 \to \phi K^{*0}$, where $K^{*0} \to K^+\pi^-$, are found to be negligible.

An unbinned maximum likelihood fit is performed to the decay time, $t$, and the three helicity angles, $\Omega = \{\theta_1, \theta_2, \Phi\}$, of the selected $B_s^0 \to \phi\phi$ candidates, each of which is reassigned a signal *sPlot* weight based on the four-kaon invariant mass, $m_{KKKK}$ [19, 20]. The probability density function (PDF) consists of signal components, which include detector resolution and acceptance effects, and are factorised into separate terms for the decay time and the angular observables.

The $B_s^0$ decay into the $K^+K^-K^+K^-$ final state can proceed via combinations of intermediate vector ($\phi$) and scalar ($f_0(980)$) resonances and scalar non-resonant $K^+K^-$ pairs. Thus the total decay amplitude is a coherent sum of $P$-wave (vector-vector), $S$-wave (vector-scalar) and $SS$-wave (scalar-scalar) contributions. The differential decay rate of the decay time and helicity angles is described by a sum of 15 terms, corresponding to

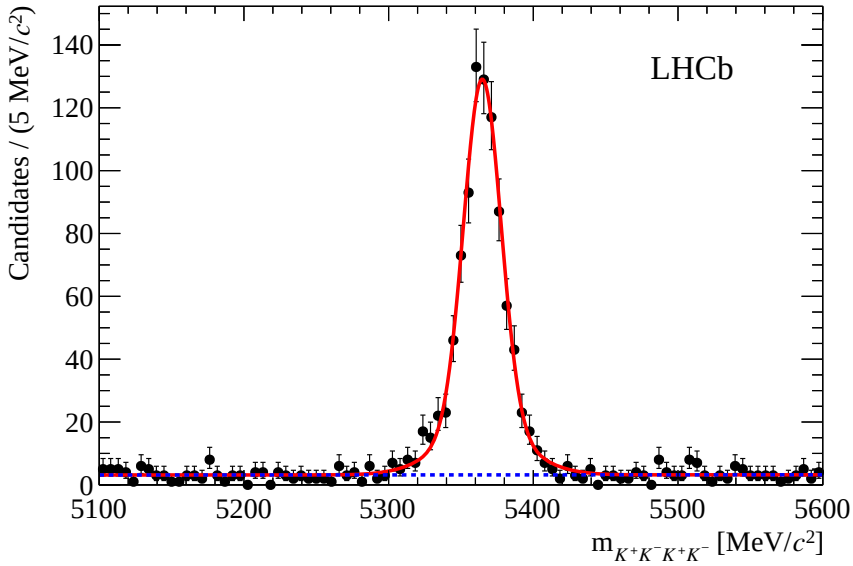


Figure 1: Invariant $K^+K^-K^+K^-$ mass distribution for selected $B_s^0 \to \phi\phi$ candidates. The total fit (solid line) consists of a double Gaussian signal component together with an exponential background (dotted line).

five polarisation amplitudes and their interference terms,

$$\frac{\mathrm{d}^4\Gamma}{\mathrm{d}\cos\theta_1\,\mathrm{d}\cos\theta_2\,\mathrm{d}\Phi\,\mathrm{d}t} \propto \sum_{i=1}^{15} K_i(t) f_i(\Omega)\,. \tag{1}$$

The angular functions $f_i(\Omega)$ for the $P$-wave terms are derived in Ref. [21] and the helicity angles of the two $\phi$ mesons are randomly assigned to $\theta_1$ and $\theta_2$. The time-dependent functions $K_i(t)$ can be written as [21]

$$K_i(t) = N_i e^{-\Gamma_s t}[c_i \cos(\Delta m_s t) + d_i \sin(\Delta m_s t) + a_i \cosh(\tfrac{1}{2}\Delta\Gamma_s t) + b_i \sinh(\tfrac{1}{2}\Delta\Gamma_s t)], \tag{2}$$

where $\Delta\Gamma_s = \Gamma_\mathrm{L} - \Gamma_\mathrm{H}$ is the decay width difference between the light (L) and heavy (H) $B_s^0$ mass eigenstates, $\Gamma_s$ is the average decay width, $\Gamma_s = (\Gamma_\mathrm{L} + \Gamma_\mathrm{H})/2$, and $\Delta m_s$ is the $B_s^0$-$\overline{B}_s^0$ oscillation frequency. The coefficients $N_i$, $a_i$, $b_i$, $c_i$ and $d_i$ can be expressed in terms of $\phi_s$ and the magnitudes, $|A_i|$, and phases, $\delta_i$, of the five polarisation amplitudes at $t = 0$. The three $P$-wave amplitudes, denoted by $A_0, A_\parallel, A_\perp$, are normalised such that $|A_0|^2 + |A_\parallel|^2 + |A_\perp|^2 = 1$, with the strong phases $\delta_1$ and $\delta_2$ defined as $\delta_1 = \delta_\perp - \delta_\parallel$ and $\delta_2 = \delta_\perp - \delta_0$. The $S$ and $SS$-wave amplitudes and their corresponding phases are denoted by $A_S$, $A_{SS}$ and $\delta_S$, $\delta_{SS}$, respectively. For a $B_s^0$ meson produced at $t = 0$, the coefficients in Eq. 2 and the angular functions $f_i(\theta_1, \theta_2, \Phi)$ are given in Table 1, where $\delta_{2,1} = \delta_2 - \delta_1$. Assuming that $CP$ violation in mixing and direct $CP$ violation are negligible, the differential distribution for a $\overline{B}_s^0$ meson is obtained by changing the sign of the coefficients

Table 1: Coefficients of the time-dependent terms and angular functions defined in Eqs. 1 and 2. Amplitudes are defined at $t = 0$.

| $i$ | $N_i$ | $a_i$ | $b_i$ | $c_i$ | $d_i$ | $f_i$ |
|---|---|---|---|---|---|---|
| 1 | $\lvert A_0\rvert^2$ | 1 | $-\cos\phi_s$ | 0 | $\sin\phi_s$ | $4\cos^2\theta_1\cos^2\theta_2$ |
| 2 | $\lvert A_\parallel\rvert^2$ | 1 | $-\cos\phi_s$ | 0 | $\sin\phi_s$ | $\sin^2\theta_1\sin^2\theta_2(1+\cos 2\Phi)$ |
| 3 | $\lvert A_\perp\rvert^2$ | 1 | $\cos\phi_s$ | 0 | $-\sin\phi_s$ | $\sin^2\theta_1\sin^2\theta_2(1-\cos 2\Phi)$ |
| 4 | $\lvert A_\parallel\rvert\lvert A_\perp\rvert$ | 0 | $-\cos\delta_1\sin\phi_s$ | $\sin\delta_1$ | $-\cos\delta_1\cos\phi_s$ | $-2\sin^2\theta_1\sin^2\theta_2\sin 2\Phi$ |
| 5 | $\lvert A_\parallel\rvert\lvert A_0\rvert$ | $\cos(\delta_{2,1})$ | $-\cos(\delta_{2,1})\cos\phi_s$ | 0 | $\cos(\delta_{2,1})\sin\phi_s$ | $\sqrt{2}\sin 2\theta_1\sin 2\theta_2\cos\Phi$ |
| 6 | $\lvert A_0\rvert\lvert A_\perp\rvert$ | 0 | $-\cos\delta_2\sin\phi_s$ | $\sin\delta_2$ | $-\cos\delta_2\cos\phi_s$ | $-\sqrt{2}\sin 2\theta_1\sin 2\theta_2\sin\Phi$ |
| 7 | $\lvert A_{SS}\rvert^2$ | 1 | $-\cos\phi_s$ | 0 | $\sin\phi_s$ | $\frac{4}{9}$ |
| 8 | $\lvert A_S\rvert^2$ | 1 | $\cos\phi_s$ | 0 | $-\sin\phi_s$ | $\frac{4}{3}(\cos\theta_1+\cos\theta_2)^2$ |
| 9 | $\lvert A_S\rvert\lvert A_{SS}\rvert$ | 0 | $\sin(\delta_S-\delta_{SS})\sin\phi_s$ | $\cos(\delta_{SS}-\delta_S)$ | $\sin(\delta_{SS}-\delta_S)\cos\phi_s$ | $\frac{8}{3\sqrt{3}}(\cos\theta_1+\cos\theta_2)$ |
| 10 | $\lvert A_0\rvert\lvert A_{SS}\rvert$ | $\cos\delta_{SS}$ | $-\cos\delta_{SS}\cos\phi_s$ | 0 | $\cos\delta_{SS}\sin\phi_s$ | $\frac{8}{3}\cos\theta_1\cos\theta_2$ |
| 11 | $\lvert A_\parallel\rvert\lvert A_{SS}\rvert$ | $\cos(\delta_{2,1}-\delta_{SS})$ | $-\cos(\delta_{2,1}-\delta_{SS})\cos\phi_s$ | 0 | $\cos(\delta_{2,1}-\delta_{SS})\sin\phi_s$ | $\frac{4\sqrt{2}}{3}\sin\theta_1\sin\theta_2\cos\Phi$ |
| 12 | $\lvert A_\perp\rvert\lvert A_{SS}\rvert$ | 0 | $-\cos(\delta_2-\delta_{SS})\sin\phi_s$ | $\sin(\delta_2-\delta_{SS})$ | $-\cos(\delta_2-\delta_{SS})\cos\phi_s$ | $-\frac{4\sqrt{2}}{3}\sin\theta_1\sin\theta_2\sin\Phi$ |
| 13 | $\lvert A_0\rvert\lvert A_S\rvert$ | 0 | $-\sin\delta_S\sin\phi_s$ | $\cos\delta_S$ | $-\sin\delta_S\cos\phi_s$ | $\frac{8}{\sqrt{3}}\cos\theta_1\cos\theta_2$ $\times(\cos\theta_1+\cos\theta_2)$ |
| 14 | $\lvert A_\parallel\rvert\lvert A_S\rvert$ | 0 | $\sin(\delta_{2,1}-\delta_S)\sin\phi_s$ | $\cos(\delta_{2,1}-\delta_S)$ | $\sin(\delta_{2,1}-\delta_S)\cos\phi_s$ | $\frac{4\sqrt{2}}{\sqrt{3}}\sin\theta_1\sin\theta_2$ $\times(\cos\theta_1+\cos\theta_2)\cos\Phi$ |
| 15 | $\lvert A_\perp\rvert\lvert A_S\rvert$ | $\sin(\delta_2-\delta_S)$ | $\sin(\delta_2-\delta_S)\cos\phi_s$ | 0 | $-\sin(\delta_2-\delta_S)\sin\phi_s$ | $-\frac{4\sqrt{2}}{\sqrt{3}}\sin\theta_1\sin\theta_2$ $\times(\cos\theta_1+\cos\theta_2)\sin\Phi$ |

$c_i$ and $d_i$. The PDF is invariant under the transformation $(\phi_s, \Delta\Gamma_s, \delta_\parallel, \delta_\perp, \delta_S, \delta_{SS}) \to (\pi-\phi_s, -\Delta\Gamma_s, -\delta_\parallel, \pi-\delta_\perp, -\delta_S, -\delta_{SS})$. This two-fold ambiguity is resolved in the fit as Gaussian constraints are applied for the $B_s^0$ average decay width and decay width difference to the values measured in $B_s^0 \to J/\psi\phi$ decays, $\Gamma_s = 0.663 \pm 0.008$ ps$^{-1}$ and $\Delta\Gamma_s = 0.100 \pm 0.017$ ps$^{-1}$, with a correlation coefficient $\rho(\Delta\Gamma_s, \Gamma_s) = -0.39$ [6]. Similarly, the $B_s^0$ oscillation frequency $\Delta m_s$ is constrained to the value $\Delta m_s = 17.73 \pm 0.05$ ps$^{-1}$ [22].

A correction factor is multiplied to the interference terms in Table 1 between the $P$ and $S$-wave (and the $P$ and $SS$-wave) contributions to account for the finite $m_{KK}$ mass window considered in the amplitude integration. This factor is calculated from the interference between the different $m_{KK}$ lineshapes of the vector and scalar contributions. The validity of the fit model has been extensively tested using simulated data samples.

The acceptance as a function of the helicity angles is not completely uniform due to the forward geometry of the detector and the momentum cuts placed to the final state particles. A three-dimensional acceptance function is determined using simulation. The acceptance factors are included in the fit as a normalisation of the PDF for each of the angular terms. The acceptance function varies by less than 20% across the phase-space.

The event reconstruction, trigger and offline selections introduce a decay time dependent acceptance. In particular for short decay times, the acceptance vanishes due to the trigger, which requires tracks with significant displacement from any PV. Therefore, the decay time acceptance is determined using simulation and incorporated by multiplying the signal PDF with a binned acceptance histogram. The fractions of different triggers are found to be in agreement between data and simulation.

The parameters of a double Gaussian function used to model the decay time resolution are determined from simulation studies. A single Gaussian function with a resolution of 40 fs is found to have a similar effect on physics parameters and is applied to the data fit.

The $\phi_s$ measurement requires that the meson flavour be tagged as either a $B_s^0$ or $\overline{B}_s^0$ meson at production. To achieve this, both the opposite side (OS) and same side kaon (SSK) flavour tagging methods are used [23, 24]. In OS tagging the $\bar{b}$-quark hadron produced in association with the signal $b$-quark is exploited through the charge of a muon or electron produced in semileptonic decays, the charge of a kaon from a subsequent charmed hadron decay, and the momentum-weighted charge of all tracks in an inclusively reconstructed decay vertex. The SSK tagging makes use of kaons formed from the $s$-quark produced in association with the $B_s^0$ meson. The kaon charge identifies the flavour of the signal $B_s^0$ meson.

The event-by-event mistag is the probability that the decision of the tagging algorithm is incorrect and is determined by a neural network trained on simulated events and calibrated with control samples [23]. The value of the event-by-event mistag is used in the fit as an observable and the uncertainties on the calibration parameters are propagated to the statistical uncertainties of the physics parameters, following the procedure described in Ref. [6]. For events tagged by both the OS and SSK methods, a combined tagging decision is made. The total tagging power is $\varepsilon_{tag}\mathcal{D}^2 = (3.29 \pm 0.48)\%$, with a tagging efficiency of $\varepsilon_{tag} = (49.7 \pm 5.0)\%$ and a dilution $\mathcal{D} = (1 - 2\omega)$ where $\omega$ is the average mistag probability. Untagged events are included in the analysis as they increase the sensitivity to $\phi_s$ through the $b_i$ terms in Eq. 2.

The total $S$-wave fraction is determined to be $(1.6\,^{+2.4}_{-1.2})\%$ where the double $S$-wave contribution $A_{SS}$ is set to zero, since the fit shows little sensitivity to $A_{SS}$. A fit to the two-dimensional mass, $m_{KK}$, for both kaon pairs, where background is subtracted using sidebands is performed and yields a consistent $S$-wave fraction of $(2.1 \pm 1.2)\%$.

The results of the fit for the main observables are shown in Table 2. Figure 2 shows the distributions for the decay time and helicity angles with the projections for the best fit PDF overlaid. The likelihood profile for the $CP$-violating weak phase $\phi_s$, shown in Fig. 3, is not parabolic. To obtain a confidence level a correction is applied due to a small under-coverage of the likelihood profile using the method described in Ref. [25]. Including systematic uncertainties (discussed below) and assuming the values of the polarisation amplitudes and strong phases observed in data, an interval of $[-2.46, -0.76]$ rad at 68% confidence level is obtained for $\phi_s$. The polarisation amplitudes and phases, shown in Table 2, differ from those reported in Ref. [9] as $\phi_s$ is not constrained to zero.

The uncertainties related to the calibration of the tagging and the assumed values of $\Gamma_s$, $\Delta\Gamma_s$ and $\Delta m_s$ are absorbed into the statistical uncertainty, described above. Systematic uncertainties are determined and the sum in quadrature of all sources is reported in Table 2 for each observable. To check that the background is properly accounted for, an additional fit is performed where the angular and time distributions are parameterised using the $B_s^0$ mass sidebands. This gives results in agreement with those presented here and no further systematic uncertainty is assigned. The uncertainty due to the modelling of the $S$-wave component is evaluated by allowing the $SS$-wave component to vary in

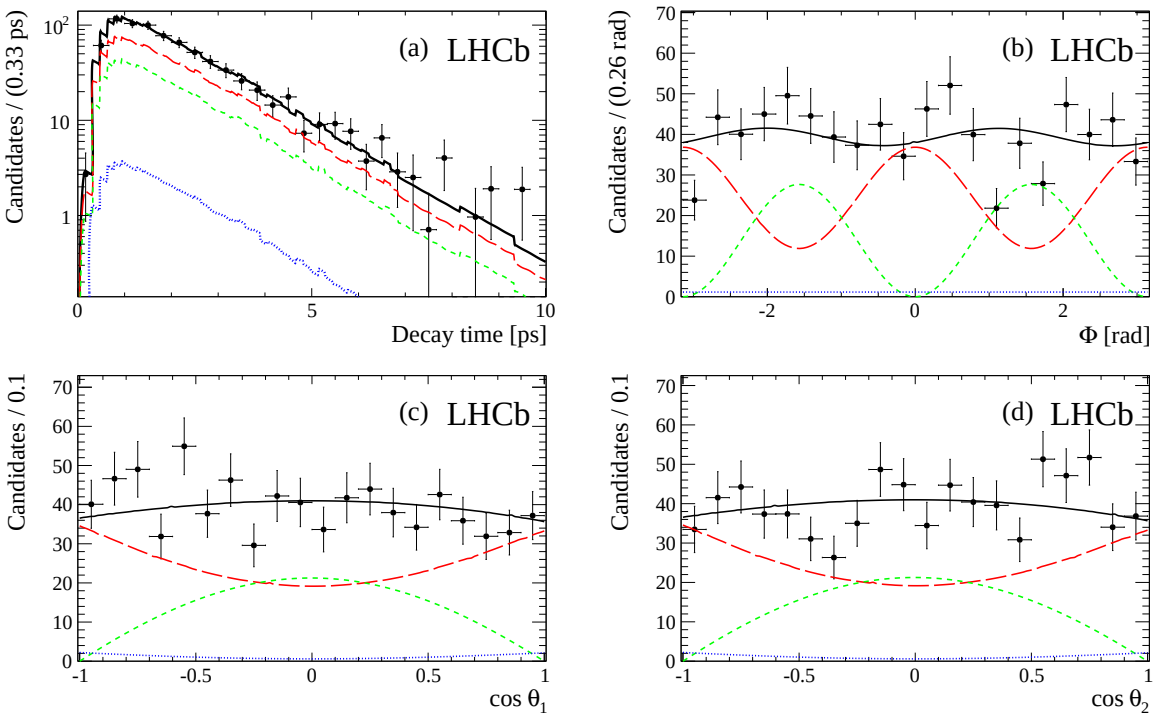


Figure 2: One-dimensional projections of the $B_s^0 \to \phi\phi$ fit for (a) decay time, (b) helicity angle $\Phi$ and the cosine of the helicity angles (c) $\theta_1$ and (d) $\theta_2$. The data are marked as points, while the solid lines represent the projections of the best fit. The *CP*-even *P*-wave, the *CP*-odd *P*-wave and *S*-wave components are shown by the long dashed, short dashed and dotted lines, respectively.

the fit. The difference between the two fits leads to the dominant uncertainty on $\phi_s$ of 0.20 rad. The systematic uncertainty due to the decay time acceptance is found by taking the difference in the values of fitted parameters between the nominal fit, using a binned time acceptance, and a fit in which the time acceptance is explicitely paramaterised. This

Table 2: Fit results with statistical and systematic uncertainties. A 68% statistical confidence interval is quoted for $\phi_s$. Amplitudes are defined at $t = 0$.

| Parameter | Value | $\sigma_{\text{stat.}}$ | $\sigma_{\text{syst.}}$ |
|---|---|---|---|
| $\phi_s$[rad] (68 % CL) | | $[-2.37, -0.92]$ | 0.22 |
| $\lvert A_0\rvert^2$ | 0.329 | 0.033 | 0.017 |
| $\lvert A_\perp\rvert^2$ | 0.358 | 0.046 | 0.018 |
| $\lvert A_{\text{S}}\rvert^2$ | 0.016 | $^{+0.024}_{-0.012}$ | 0.009 |
| $\delta_1$ [rad] | 2.19 | 0.44 | 0.12 |
| $\delta_2$ [rad] | $-1.47$ | 0.48 | 0.10 |
| $\delta_{\text{S}}$ [rad] | 0.65 | $^{+0.89}_{-1.65}$ | 0.33 |

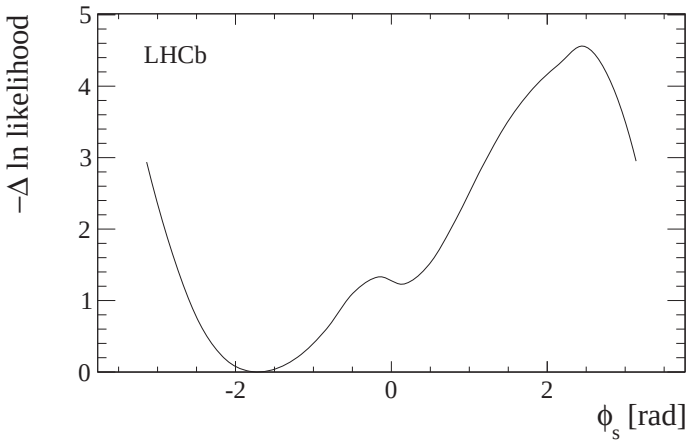


Figure 3: Negative $\Delta$ln likelihood scan of $\phi_s$. Only the statistical uncertainty is included.

is found to be 0.09 rad for $\phi_s$. Possible differences in the simulated decay time resolution compared to the data are studied by varying the resolution according to the discrepancies observed in the $B_s^0 \to J/\psi\phi$ analysis [6]. This leads to a systematic uncertainty of 0.01 rad for $\phi_s$. The distributions of maximum $p_{\rm T}$ and $\chi^2$/ndf of the final state tracks and the $p_{\rm T}$ and $\eta$ of the $B_s^0$ candidate are reweighted to better match the data. From this, the angular acceptance is recalculated, leading to small changes in the results (0.02 rad for $\phi_s$), which are assigned as systematic uncertainty. Biases in the fit method are studied using simulated pseudo-experiments that lead to an uncertainty of 0.02 rad for $\phi_s$. Further small systematic uncertainties (0.02 rad for $\phi_s$) are due to the limited number of events in the simulation sample used for the determination of the angular acceptance and to the choice of a single versus a double Gaussian function for the mass PDF, which is used to assign the signal weights. The total systematic uncertainty on $\phi_s$ is 0.22 rad, significantly smaller than the statistical uncertainty.

In summary, we present the first study of *CP* violation in the decay time distribution of hadronic $B_s^0 \to \phi\phi$ decays. The *CP*-violating phase, $\phi_s$, is restricted to the interval of $[-2.46, -0.76]$ rad at 68% C.L. The p-value of the Standard Model prediction [8] is 16%, taking the values of the strong phases and polarisation amplitudes observed in data and assuming that systematic uncertainties are negligible. The precision of the $\phi_s$ measurement is dominated by the statistical uncertainty and is expected to improve with larger LHCb data sets.

# Acknowledgements

We express our gratitude to our colleagues in the CERN accelerator departments for the excellent performance of the LHC. We thank the technical and administrative staff at the LHCb institutes. We acknowledge support from CERN and from the national agencies:

CAPES, CNPq, FAPERJ and FINEP (Brazil); NSFC (China); CNRS/IN2P3 and Region Auvergne (France); BMBF, DFG, HGF and MPG (Germany); SFI (Ireland); INFN (Italy); FOM and NWO (The Netherlands); SCSR (Poland); ANCS/IFA (Romania); MinES, Rosatom, RFBR and NRC "Kurchatov Institute" (Russia); MinECo, XuntaGal and GENCAT (Spain); SNSF and SER (Switzerland); NAS Ukraine (Ukraine); STFC (United Kingdom); NSF (USA). We also acknowledge the support received from the ERC under FP7. The Tier1 computing centres are supported by IN2P3 (France), KIT and BMBF (Germany), INFN (Italy), NWO and SURF (The Netherlands), PIC (Spain), GridPP (United Kingdom). We are thankful for the computing resources put at our disposal by Yandex LLC (Russia), as well as to the communities behind the multiple open source software packages that we depend on.

# References

[1] M. Bartsch, G. Buchalla, and C. Kraus, *$B \to V_L V_L$ decays at next-to-leading order in QCD*, arXiv:0810.0249.

[2] M. Beneke, J. Rohrer, and D. Yang, *Branching fractions, polarisation and asymmetries of $B \to VV$ decays*, Nucl. Phys. **B774** (2007) 64, arXiv:hep-ph/0612290.

[3] H.-Y. Cheng and C.-K. Chua, *QCD factorization for charmless hadronic $B_s$ decays revisited*, Phys. Rev. **D80** (2009) 114026, arXiv:0910.5237.

[4] M. Kobayashi and T. Maskawa, *CP violation in the renormalizable theory of weak interaction*, Prog. Theor. Phys. **49** (1973) 652; N. Cabibbo, *Unitary symmetry and leptonic decays*, Phys. Rev. Lett. **10** (1963) 531.

[5] J. Charles *et al.*, *Predictions of selected flavor observables within the Standard Model*, Phys. Rev. **D84** (2011) 033005, arXiv:1106.4041.

[6] LHCb collaboration, R. Aaij *et al.*, *Measurement of $CP$-violation and the $B_s^0$-meson decay width difference with $B_s^0 \to J/\psi K^+K^-$ and $B_s^0 \to J/\psi \pi^+\pi^-$ decays*, LHCb-PAPER-2013-002, in preparation.

[7] LHCb collaboration, R. Aaij, *et al.*, and A. Bharucha *et al.*, *Implications of LHCb measurements and future prospects*, arXiv:1208.3355, to appear in Eur. Phys. J. C.

[8] M. Raidal, *CP asymmetry in $B \to \phi K_S$ decays in left-right models and its implications for $B_s$ decays*, Phys. Rev. Lett. **89** (2002) 231803, arXiv:hep-ph/0208091.

[9] LHCb collaboration, R. Aaij *et al.*, *Measurement of the polarization amplitudes and triple product asymmetries in the $B_s^0 \to \phi\phi$ decay*, Phys. Lett. **B713** (2012) 369, arXiv:1204.2813.

[10] LHCb collaboration, A. A. Alves Jr. *et al.*, *The LHCb detector at the LHC*, JINST **3** (2008) S08005.

[11] R. Aaij *et al.*, *The LHCb trigger and its performance*, arXiv:1211.3055, submitted to JINST.

[12] T. Sjöstrand, S. Mrenna, and P. Skands, *PYTHIA 6.4 physics and manual*, JHEP **05** (2006) 026, arXiv:hep-ph/0603175.

[13] I. Belyaev *et al.*, *Handling of the generation of primary events in* Gauss*, the LHCb simulation framework*, Nuclear Science Symposium Conference Record (NSS/MIC) **IEEE** (2010) 1155.

[14] D. J. Lange, *The EvtGen particle decay simulation package*, Nucl. Instrum. Meth. **A462** (2001) 152.

[15] GEANT4 collaboration, J. Allison *et al.*, *Geant4 developments and applications*, IEEE Trans. Nucl. Sci. **53** (2006) 270; GEANT4 collaboration, S. Agostinelli *et al.*, *GEANT4: a simulation toolkit*, Nucl. Instrum. Meth. **A506** (2003) 250.

[16] M. Clemencic *et al.*, *The LHCb simulation application,* Gauss*: design, evolution and experience*, J. of Phys.: Conf. Ser. **331** (2011) 032023.

[17] M. Adinolfi *et al.*, *Performance of the LHCb RICH detector at the LHC*, arXiv:1211.6759, submitted to EPJC.

[18] L. Breiman, J. H. Friedman, R. A. Olshen, and C. J. Stone, *Classification and regression trees*, Wadsworth international group, Belmont, California, USA, 1984.

[19] M. Pivk and F. R. Le Diberder, *sPlot: a statistical tool to unfold data distributions*, Nucl. Instrum. Meth. **A555** (2005) 356, arXiv:physics/0402083.

[20] Y. Xie, *sFit: a method for background subtraction in maximum likelihood fit*, arXiv:0905.0724.

[21] C.-W. Chiang and L. Wolfenstein, *Observables in the decays of B to two vector mesons*, Phys. Rev. **D61** (2000) 074031, arXiv:hep-ph/9911338.

[22] LHCb collaboration, *Measurement of $\Delta m_s$ in the decay $B_s^0 \to D_s^-(K^+K^-\pi^-)\pi^+$ using opposite-side and same-side flavour tagging algorithms*, LHCb-CONF-2011-050.

[23] LHCb collaboration, R. Aaij *et al.*, *Opposite-side flavour tagging of B mesons at the LHCb experiment*, Eur. Phys. J. **C72** (2012) 2022, arXiv:1202.4979.

[24] LHCb collaboration, *Optimization and calibration of the same-side kaon tagging algorithm using hadronic $B_s^0$ decays in 2011 data*, LHCb-CONF-2012-033.

[25] G. J. Feldman and R. D. Cousins, *A unified approach to the classical statistical analysis of small signals*, Phys. Rev. **D57** (1998) 3873, arXiv:physics/9711021.